International Journal of Thermophysics (2021) 42:94
https://doi.org/10.1007/s10765-021-02845-6

Investigations of Electrical Resistivity and Thermal Conductivity Dependences on Growth Rate in the Al–Cu–Ti Eutectic Alloy

Necmettin Maraşlı[1] · **Ümit Bayram**[2]

Received: 1 March 2021 / Accepted: 1 April 2021 / Published online: 3 May 2021

Abstract

Directional solidification of Al–Cu–Ti (Al–33wt%Cu–0.1wt%Ti) eutectic alloy was done with a growth rate range ($V = 8.58$ to 2038.65 $\mu m \cdot s^{-1}$) at a temperature gradient of 6.45 $K \cdot mm^{-1}$ using Bridgman-type directional solidification furnace. The measurements of thermal conductivity (K) and electrical resistivity (ρ) for the Al–Cu–Ti alloy solidified with the different values of V were made by the longitudinal heat flow method (LHFM) and DC four-point probe technique (FPPT). While the highest values of K and ρ were determined to be 236.04 $W \cdot K^{-1} \cdot m^{-1}$ and 5.91×10^{-8} Ωm, respectively, at 8.58 $\mu m \cdot s^{-1}$, the lowest values of K and ρ were obtained to be 199.82 $W \cdot K^{-1} \cdot m^{-1}$ and 12.11×10^{-8} Ωm, respectively, at 2038.65 $\mu m \cdot s^{-1}$. The K and ρ dependences on V were obtained to be $K = 259.96 \times V^{-0.032}$ and $\rho = 4.47 \times 10^{-8} V^{0.13}$ from linear regression analysis. The fusion enthalpy (ΔH) and specific heat difference between solid and liquid (ΔC_P) for the Al–Cu–Ti were also determined to be 222.69 $J \cdot g^{-1}$ and 0.266 $Jg^{-1} \cdot K^{-1}$, respectively, by means of differential scanning calorimetry (DSC).

Keywords Aluminum alloys · Directional solidification · Electrical resistivity · Microstructure · Thermal conductivity

✉ Necmettin Maraşlı
nmarasli@yildiz.edu.tr

Ümit Bayram
umitbayram14@gmail.com

[1] Department of Metallurgical and Materials Engineering, Faculty of Chemistry and Metallurgical Engineering, Yıldız Technical University, 34210 İstanbul, Turkey

[2] Central Research Facility, Abdullah Gül University, 38080 Kayseri, Turkey

1 Introduction

The development of new workable aluminum-based light alloys is a key issue in current materials science. In the aluminum industry, the most used casting alloy is the Al–Cu alloys. The Al–Cu alloys are ubiquitous in technical applications: they are the main components for screw machine products, truck frames, aircraft structures, jet engine impellers, and aircraft engine cylinder heads [1–3].

The solidification is the phase transformation from liquid to solid. During the solidification, the atomic mass transfers occur from liquid to solid, atoms become together to form phases, and then phases become together to form bulk solid materials. The rate of mass transfer plays a critical role to control the structural, physical, and mechanical properties of materials. Thus, the physical and mechanical properties of materials can be controlled by understanding the mechanism of solidification [1].

It has known that the change in microstructure of metallic materials directly affects its mechanical, physical and corrosion properties. In alloys, especially eutectic alloys, the microstructures, the phase dimensions, and grain size directly depend on solidification parameters (X, composition of alloy; G, temperature gradient; and V, growth rate). In other words, it is possible to determine the microstructures and hence other properties of the alloys by controlling the solidification parameters independently.

Basic alloys for engineering is also the eutectic alloys due to their low melting point and superior casting capability [2, 3]. In the casting industry, the eutectic composition or near-eutectic composition is generally preferred [2]. During the directional solidification of binary or ternary eutectics, the well-aligned regular structures consisting of fibrous (rod-like) or lamellar constituents are produced and substantial increases in high-temperature strength, fracture properties, or creep resistance over those of conventionally cast alloys can be obtained with such structures [4]. For the first time, the turbine blades were produced by the directional solidification method [5]. The relationship between alloys and their microstructure and process conditions are identified by this method. Additionally, to improve both individual and combinations of properties in conventional Al alloys, such as thermal stability and elastic stiffness, by means of nonconventional alloy additions that are actually detrimental at normal rates of solidification, the molten aluminum alloys was rapid quenched [6].

The most effective control parameter for directional solidification is the cooling rate ($T' = \mathrm{d}T/\mathrm{d}t = V \times G$) [7–22]. Thus, the physical and mechanical properties of directionally solidified alloys depend on the growth rate.

The ρ and K parameters for the materials play a critical role in controlling the performance and stability of materials and they are the main fundamental properties of materials, such as density, melting point, entropy, and crystal structure parameters. The ρ and K for any kinds of alloy depend on V as well as T and X. Determination of ρ and K are a valuable tool for the study of transport mechanisms of alloys. Dependences of K and ρ on V have just theoretically known, but there is not enough sufficient formulation to show the relationships between

them. Especially there is no more study on variations of K with V for binary or multicomponent alloys.

Recently, the effects of V on K and ρ in the Al–Cu–Ni eutectic system have been investigated [22]. Based on the recent study [22], one wondered what the effects of V on K and ρ and whether the effect depends on the types of alloying elements in the Al–Cu–Ti? To find answer to these questions, it was decided to measure the variations of K and ρ with V in the Al–Cu–Ti.

2 Materials and Methods

The experimental processes for solidifying of the Al–Cu–Ti eutectic alloy are group in steps of alloy solidification with the different growth rates, determination of solidification and microstructure parameters, and the measurements of electrical resistivity and thermal conductivity. The explanation of the experimental processes are outlined as follows.

2.1 Solidification of Alloy with Different Growth Rates

In the present study, the alloying element of Ti was added into Al–33wt%Cu eutectic alloy in the limit of solid solubility of solid Ti in the solid Al in order to grow the Al_{α} and $CuAl_2$ (θ) eutectic phases from the Al–Cu–Ti. The Al–Cu–Ti molten alloy was prepared from 4N and 3N purity of Al, Cu and % Ni, respectively, under vacuum and then poured into graphite pots, held in a hot filling furnace, and preheated up to 50 K above the melting point of eutectic alloy. The Al–Cu–Ti molten alloy into graphite pot that is held in a hot filling furnace was solidified from bottom to top to get completely full specimens.

Each specimen was then re-melted at a temperature of 150 K above its melting temperature in a Bridgman-type furnace as shown in Fig. 1. After stabilizing thermal condition, the molten alloy was grown about 10 or 15 cm by pulling it downwards with a constant pulling speed and then quenched rapidly by pulling it down into the water reservoir [20–22].

The high growth rate was reached to be 2056.68 $\mu m \cdot s^{-1}$ with a specially constructed driving system in the present work. The pulling rate versus the applied voltage and growth rate versus the pulling rate for the driving system were determined and they are given in Table 1. The directional solidification of Al–Cu–Ti with the different V values (from 8.58 $\mu m \cdot s^{-1}$ to 2038.65 $\mu m \cdot s^{-1}$) was done at 4.65 $K \cdot mm^{-1}$ by using the driving system. The experimental procedures and Bridgman-type furnace details are outlined in References [20–22].

2.2 Determination of Solidification and Microstructure Parameters

0.25 mm thick and metal sheathed K-type thermocouples were used to measure the temperature difference (ΔT) into the sample within a space of 4–5 mm (ΔX). All the thermocouple's ends were connected to a data logger via computer.

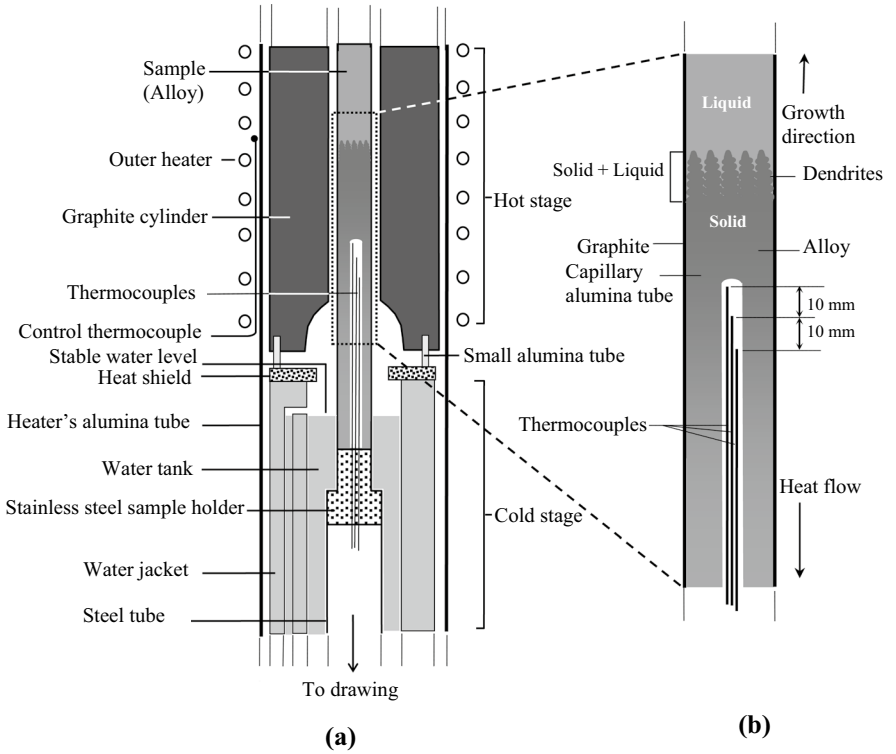

Fig. 1 The details of the Bridgman-type directional solidification; (a) Hot and cold stages of the furnace, (b) the details of sample

Table 1 Applied voltage versus pulling rates and pulling rates versus growth rates obtained with constructed driving system

Applied DC voltage (V)	Pulling Rate ($\mu m \cdot s^{-1}$)	Growth Rate for the Al–Cu–Ti alloy ($\mu m \cdot s^{-1}$)
1.0	1012.26	490.81
2.1	2085.47	1018.16
2.9	3057.53	1497.42
3.8	4174.32	2038.65

Thus, a data logger recorded the cooling rate during the growth. The values of ΔT and the time required for the solid-liquid interface to pass the distance between two thermocouples (Δt) were read from data logger record. Thus, the values of $V = \Delta X/\Delta t$ and temperature gradient into liquid ($G = \Delta T/\Delta X$) for each sample were determined from the measured ΔT and Δt values and known ΔX value.

The values of Δt was read from data logger record. Thus, the value of $V = \Delta X/\Delta t$ for each sample was determined using the measured values of Δt and ΔX. The estimated error in the measurements of G can be determined with a fractional total uncertainty in G, which can be expressed as

$$\left|\frac{\Delta G}{G}\right| = \left|\frac{\Delta T^*}{\Delta T}\right| + \left|\frac{\Delta X^*}{\Delta X}\right|, \tag{1}$$

where ΔT^* is the uncertainty in the temperature measurement, ΔX^* is the uncertainty in the distance measurement, ΔT is the temperature difference between fixed two points, and ΔX is the distance between fixed two thermocouples.

The distance between two thermocouples was measured from the photographs of the thermocouple's positions to be 4–5 mm with an accuracy of ± 5 μm. The fractional uncertainty in the measurement of the fixed distances is about 0.2 %.

To determine the uncertainty in the temperature measurements, the thermocouples were calibrated by detecting the melting point of binary alloy. The uncertainty in the temperature measurements (ΔT^*) at the melting temperature of binary alloys was about 1 K. The value of $\Delta T = T_1 - T_2$ was about 80–100 K. The uncertainty in the temperature measurements is about 1.3 %. Therefore, the total fractional uncertainty in the measurements of temperature gradient is approximately 1.5 %.

The estimated error in the measurements of V can be expressed as

$$\left|\frac{\Delta V}{V}\right| = \left|\frac{\Delta X^*}{\Delta X}\right| + \left|\frac{\Delta t^*}{\Delta t}\right|, \tag{2}$$

where Δt^* is the uncertainty in the time measurements, Δt is the time taken for the solid–liquid interface to pass through the two thermocouples. The fractional uncertainty in the measurements of the distances was about 0.3 %. The time required for the solid-liquid interface to pass the distance between two thermocouples is about 80 s at higher growth rates and the uncertainty in the time measurements is about 1.3 %. Thus, total uncertainty in the V measurement is approximately 2 %.

Some routine metallographic processes were carried out to reveal the microstructure of samples. For these metallographic processes, the transverse sections of samples, cut into a length of 15 mm, were flatted with SiC papers, cold mounted, and then polished. After polishing, the samples were etched with a Keller's micro etchant for 40–45 s. Some micrographs of microstructures taken with a LEO scanning electron microscopy (SEM) for Al–33wt%Cu–0.1wt%Ti alloy solidified with different growth rates are shown in Fig. 2.

The λ values obtained from the transverse sections are more reliable than that of longitudinal section of the samples [10], and the linear intersection method [10] was used to determine the lamellar spacing (λ) from the micrographs of microstructures. Any increments in the growth rate causes the Al–Cu–Ti has fine lamellar eutectic microstructure as shown in Fig. 2. In the measurements of microstructure parameters, 30–40 values of λ for each temperature gradient were measured to increase statistical sensitivity. So, the statistical error in the measurements of the microstructures was minimized and is given in Table 2.

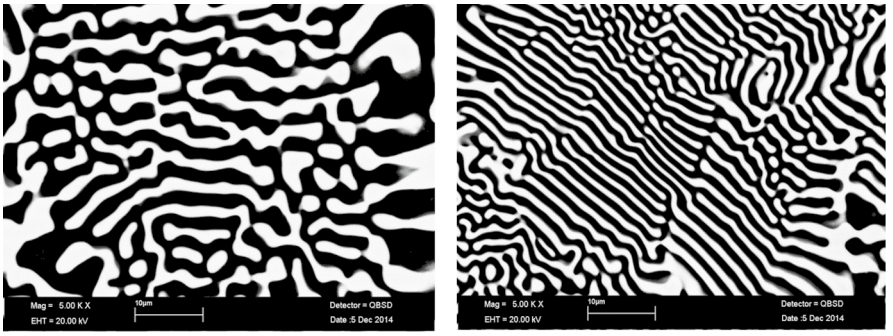

(a) V= 8.58 µm s^{-1} **(b)** V= 42.85 µm s^{-1}

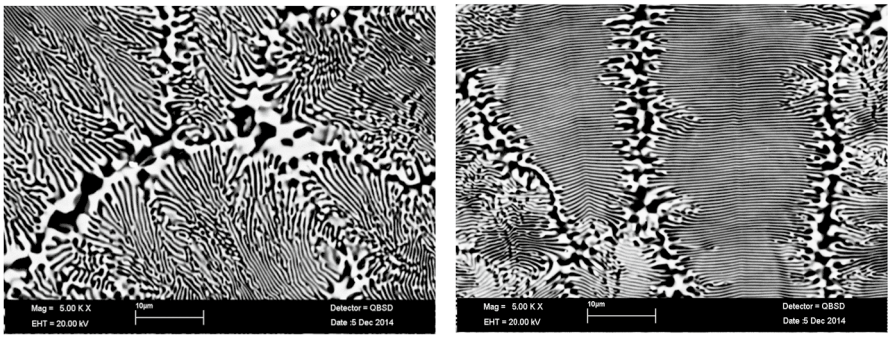

(c) V=1018.16 µm s^{-1} **(d)** V=2038.65 µm s^{-1}

Fig. 2 Typical SEM images for the directional solidified Al–33 wt% Cu–0.1 wt% Ti eutectic alloy at a constant temperature gradient of 4.65 K·mm^{-1} with different growth rates

2.3 Electrical Resistivity Measurements

In literature, many works on ρ measurements of pure metals are present, but the studies on determination of ρ value for multicomponent systems are very limited. In alloys, the value of ρ depends on temperature, dimension of phases, grain size, plastic deformation, heat treatment conditions, and composition of alloy [23].

The FPPT is the most widely used technique for electrical resistivity measurement of materials. A FPP measurement is performed by making four electrical contacts to a sample surface. The outer and inner probe pairs are used to measure source current and to measure voltage, respectively. The measured four-point resistance does not contain contributions from the contact resistance between the sample and the electrodes. The electrical resistivity (ρ) is determined by loading a direct current, I, through the outer probes and measuring the voltage drop, ΔV, between the inner probes. The space between the probes was 1 mm.

The electrical resistivity is expressed as

Table 2 The values of G, V, λ, ρ, and K for the directional solidified Al–33 wt% Cu–0.1 wt% Ti eutectic alloy

Alloy (wt %)	Temperature gradient, G ($K \cdot mm^{-1}$)	Growth rate V ($\mu m \cdot s^{-1}$)	Lamellar spacing λ (μm)	Electrical resistivity, $\rho \times 10^{-8}$ (Ωm)	Thermal conductivity, K ($W \cdot K^{-1} \cdot m^{-1}$)	Lorentz number, $L \times 10^{-8}$ ($W \cdot \Omega \cdot K^{-2}$)
Al–33Cu–0.1Ti	4.65 ± 0.07	8.58 ± 0.17	3.97 ± 0.48	5.91 ± 0.30	236.04 ± 21.24	4.65
		42.85 ± 0.86	2.35 ± 0.29	7.18 ± 0.36	232.39 ± 20.92	5.56
		83.42 ± 1.67	1.63 ± 0.19	7.89 ± 0.40	230.74 ± 20.76	6.07
		164.15 ± 3.28	0.87 ± 0.12	9.02 ± 0.45	224.02 ± 20.16	6.74
		490.81 ± 9.82	**0.68 ± 0.10**	**10.14 ± 0.51**	**221.43 ± 19.93**	**7.48**
		1018.16 ± 20.36	**0.59 ± 0.08**	**10.78 ± 0.54**	**209.80 ± 18.88**	**7.54**
		1497.42 ± 29.95	**0.49 ± 0.06**	**11.35 ± 057**	**202.24 ± 18.20**	**7.65**
		2038.65 ± 40.76	**0.44 ± 0.05**	**12.11 ± 0.61**	**199.82 ± 17.98**	**8.07**

ρ: The average values of the electrical resistivity measured from the longitudinal section

Bold values indicate measured experimental values for high growth rates

$$\rho = \mathrm{RCF}\frac{\Delta V_{\mathrm{measured}}}{I_{\mathrm{measured}}}, \tag{3}$$

where RCF is the resistivity correction factor. RCF takes the size of the test structure, the thickness of the material, the size of the electrodes, and the position of the electrodes with respect to the boundary of the test structure into account [24]. RCF for the sample is calculated to be 0.364 cm [25].

The measurements of electrical resistivity were conducted at 300 K on circular shape samples with a typical diameter of 1.25 cm, using a standard *FPPT*. The measuring unit was interfaced with a PC for the online data acquisition and processing. A Keithley 2400 source meter was used to provide constant current of 1 A and the potential drop was detected by a Keithley 2700 multimeter. Platinum wires with a diameter of 0.5 mm were employed as current and potential electrodes. The voltage drop and the current were detected and the electrical resistivity was determined from Eq. (3).

In order to examine the influence of V on ρ, the value of ρ for the Al–Cu–Ti alloy directionally solidified with the different V values was measured with the DC FPPT [24]. The experimental error in the ρ measurements is about 5 % [25].

2.4 Thermal Conductivity Measurement

The K value is the basic property of materials. Although the values of K for metals were determined from theoretical approaches and experimental studies, the sufficient information or available data on K values for alloys are not exist. The K value for alloys changes with T and V as well as composition of alloys, X.

One of the useful techniques for measuring K value of solid is the LHFM. In the LHFM, the experimental apparatus is set up in which the flow of heat is only in the axial direction of a road specimen. Assuming heat flow is steady state and no radial heat loss or gain, K value is determined from one-dimensional Fourier–Biot heat conduction equation [26, 27]:

$$K = \frac{\overset{*}{Q}\,\Delta X}{A\,\Delta T}, \tag{4}$$

where $\overset{*}{Q}$ is the input power, A is the cross-sectional surface area of the specimen which is normal to heat flow direction, and $\Delta T = T_1 - T_2$ is the temperature difference at a distance of $\Delta X = X_1 - X_2$ into the sample, where $\Delta X = X_1 - X_2$ is the distance between two thermocouple's positions.

In the present work, an LHF apparatus, originally designed by Aksoz et al. [28], was used to measure the K values of the Al–Cu–Ti solidified with the different values of V at room temperature. The solidified cylindrical sample was cut into 30 mm length which consists of two zones: 20 mm length of sample contains one end closed alumina tube and 10 mm length of sample does not contain alumina tube. The cylindrical sample (30 mm in length) was then placed into the *LHF* apparatus. To keep the sample at a constant temperature gradient, one side of sample was heated by a hot stage and other side of sample was cooled by a cold stage. The temperature of heater and cold stage was held at constant temperature of 300 K and 253 K, respectively,

with the temperature controllers. The side surface of sample was wrapped with glass fiber blanket to get the LHF into the road specimen and stop the radial heat loss or gain. The space of between the hot stage and cold stage was 10 mm. The samples were kept under steady state condition at least 4 hour and the values of ΔT into sample and the applied current (I) and voltage drops at the ends of heater (ΔV_{heater}) were recorded with a data logger and the data acoustics via to computer, respectively for sensitive input power measurements. The values of K were calculated using the determined values of A,$\overset{*}{\text{Q}} = \text{I} \times \Delta \text{V}_{heater}$, ΔT, and ΔX from Eq. (4).

The input powers given to experimental system (heater) for without specimen ($\overset{*}{Q}_{\text{WOS}}$) and with specimen ($\overset{*}{Q}_{\text{WS}}$) were separately determined by measuring the voltage drops at the end of heater and currents passing through the heater under the steady-state conditions. Heat flow rate into rod specimen ($\overset{*}{Q}$) for steady-state condition was assumed to be the difference between the values of $\overset{*}{Q}_{\text{WS}}$ and $\overset{*}{Q}_{\text{WOS}}$ in the present work.

The estimated experimental error in the measurement of K is the sum of the fractional uncertainty of the measurements of heat flow rate, temperature difference, cross-sectional area of specimen, and thermocouple positions, which can be expressed as

$$\left|\frac{\Delta K}{K}\right| = \left|\frac{\Delta \overset{*}{Q}}{\overset{*}{Q}}\right| + \left|\frac{\Delta T}{T}\right| + \left|\frac{\Delta A}{A}\right| + \left|\frac{\Delta X}{X}\right|. \tag{5}$$

The estimated experimental error in the measurement of $\overset{*}{Q}$ is the sum of the fractional uncertainty in the measurements of $\overset{*}{Q}_{\text{WS}}$ and $\overset{*}{Q}_{\text{WOS}}$ which can be expressed as

$$\left|\frac{\Delta \overset{*}{Q}}{\overset{*}{Q}}\right| = \left|\frac{\Delta \overset{*}{Q}_{\text{WS}}}{\overset{*}{Q}_{\text{WS}}}\right| + \left|\frac{\Delta \overset{*}{Q}_{\text{WOS}}}{\overset{*}{Q}_{\text{WOS}}}\right|. \tag{6}$$

The input power is expressed as

$$\overset{*}{Q} = \Delta V_{\text{heater}} \times I, \tag{7}$$

where ΔV_{heater} and I are the potential drop at the end of hot stage (heater) and the current passing through the heater, respectively, under the steady-state condition. The fractional uncertainty in the power measurement can be expressed as

$$\left|\frac{\Delta \overset{*}{Q}}{\overset{*}{Q}}\right| = \left|\frac{\Delta \overset{*}{V}_{\text{heater}}}{\Delta V_{\text{heater}}}\right| + \left|\frac{\Delta I}{I}\right|. \tag{8}$$

The ΔV_{heater} and I were measured with a *Hewlett-Packard 34401-A* multimeter. The variations in the current reading (ΔI) were ± 0.02 A at room temperature.

The current passing through to specimen was 0.95 A at room temperature. The uncertainty in the current measurement is 2.2 % and total estimated error in the current measurement for determination of net heat transfer is about 4.4 %.

The variations in the potential drop readings (ΔV_{heater}) were ± 0.03 V at room temperature. The potential drop at the end of hot stage (ΔV_{heater}) was about 9.0 V. The uncertainty in the potential drop measurement is about 0.3 % and total estimated error in the potential drop measurements for determination of net heat transfer is about 0.6 %. Thus, the total fractional uncertainty in the heat flow rate measurements is about 5.0 %.

The temperature of the specimen was measured with K-type thermocouples. The difference of the two thermocouple readings (ΔT^*) at the same points of the specimen must be known or measured to determine the uncertainty of temperature measurement. To determine the difference of the thermocouple readings, the thermocouples were calibrated by detecting the melting point of a metallic material. The difference between the two thermocouple readings (ΔT^*) was in the range of ± 0.03–0.2 K at different temperatures [29]. The $\Delta T = T_1 - T_2$ was in the range of 1.2 K at 300 K. The estimated error in the temperature measurement into the specimen is about 2.5 %.

The fractional uncertainty in the cross-sectional surface measurement ($A = \pi r^2$) is expressed as

$$\left|\frac{\Delta A}{A}\right| = 2\left|\frac{\Delta r}{r}\right|, \tag{9}$$

where r is the radius of specimen. The radius of specimen is measured to be 4000 μm by using an optical microscope with an accuracy of ± 10 μm. Thus, the uncertainty in the measurement of radius or cross-sectional area of specimen is less than 0.5 %.

The distance between two thermocouple positions ($\Delta X = X_2 - X_1$) was also measured by using an optical microscope with an accuracy of ± 10 μm. The measured value of ΔX is about 3000 μm. The fractional uncertainty in the measurement of ΔX is about 0.3 %.

Therefore, the total experimental error in the measurement of K is determined to be 9 %.

2.5 Determinations of ΔC_p and ΔH of Fusion

The values of ΔC_{p} and ΔH were obtained from DSC trace with a heating rate of 10 K·min^{-1} up to 1000 K for the Al–Cu–Ti alloy. The ΔC_{p} is expresses as

$$\Delta C_{\text{P}} = \frac{\Delta H}{T_{\text{M}}}, \tag{10}$$

where T_{M} is the melting temperature of the alloy. Thus, ΔH and ΔC_{p} values are determined from DSC trace by determining the area under the peak and by using the values of ΔH and T_{M} from Eq. (10), respectively.

3 Results and Discussion

3.1 Microstructure Analysis

The eutectic composition of Al–Cu–Ti alloy was determined to be Al–33wt%Cu–0.1wt%Ti [30, 31] and the cooling of the Al–Cu–Ti eutectic liquid provides $L \rightarrow \alpha\text{-Al}$ (matrix phase) solution $+ \theta - Al_2Cu$ (intermetallic phase) [31]. This means that when the Al–Cu–Ti eutectic liquid is cooled to a few degrees below the eutectic temperature, solid Al_α solution and solid $\theta(Al_2Cu)$ phases can grow together from the Al–Cu–Ti liquid according to eutectic reaction.

Typical SEM micrographs for Al–Cu–Ti directionally solidified with the different V values are given in Fig. 1. EDX (Energy Dispersive X–ray) analyzer was used to identify the compositions of Al_α and Al_2Cu (θ) phases. According to EDX results shown in Fig. 3, the white and black colors are the Al_2Cu (θ) and Al_α phases, respectively.

As shown in Fig. 2, the value of λ decreases with the increasing V at 6.45 $K \cdot mm^{-1}$. The highest and the smallest λ values were determined at 8.58 $\mu m \cdot s^{-1}$ and 2038.65 $\mu m \cdot s^{-1}$, respectively, as shown in Figs. 1d and 2a.

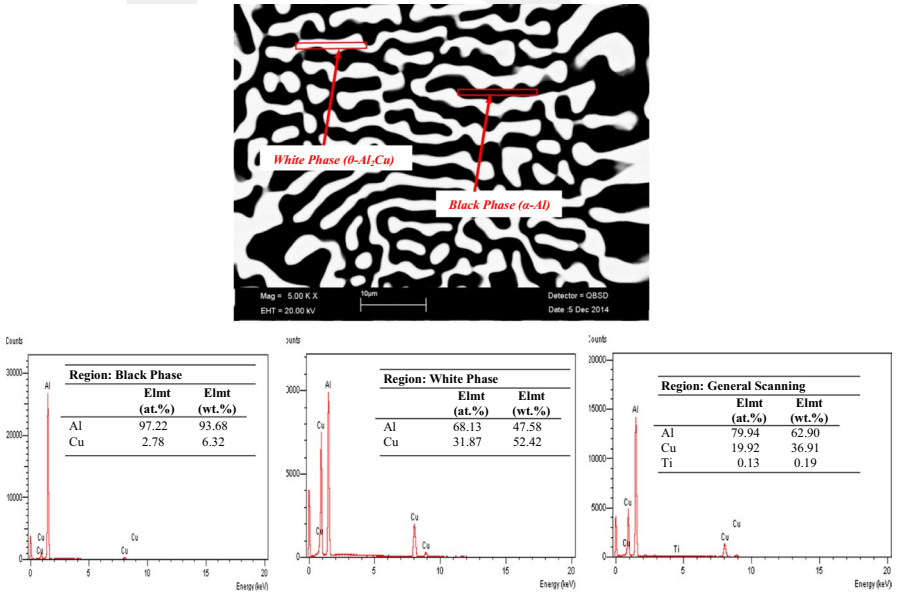

Fig. 3 The chemical composition analysis of Al–33wt% Cu–0.1wt% Ti eutectic alloy by using SEM EDX. Black phase is matrix α-Al phase and white phase is θ-Al_2Cu intermetallic phase

3.2 Variation of ρ with V

The ρ of alloy varies with V. According to eutectic growth theory [19], the λ is proportional to the inverse square root of V. As mentioned above, the ρ values for the Al Cu–Ti solidified with the different values of V were measured with the DC FPPT at room temperature, 300 K. The variations of ρ with λ and V in the form of Hall–Petch (H–P)-type equation are shown in Fig. 4. As shown in Figs. 2 and 4, the λ values and thus the grain size decrease or the number of grain boundary and interface between the Al_{α} and $CuAl_2$ phases increase with the increasing value of V. Thus, the value of ρ increases with the increasing V, while the value of λ decreases with the increasing V. Thus, the dependences of ρ on λ and V for the Al–Cu–Ti were determined in the form of H–P-type equation by assuming λ as the mean grain size as follows:

$$\rho = \left(5.77 + 2.84\,\lambda^{-1}\right) \times 10^{-8}, \tag{11}$$

$$\rho = \left(6.51 + 0.13\,V^{0.5}\right) \times 10^{-8}. \tag{12}$$

The dependences of ρ on λ and V in the form of H–P-type equation for the Al–Cu–Ti were compared with the dependences of ρ on λ and V for Al–Cu–Ni [21, 22] as shown in Fig. 4. The 2.84 and 0.13 coefficient values of λ and V for the Al–Cu–Ti are close to the 1.73 and 0.09 coefficient values of λ and V, respectively, for the Al–Cu–Ni [21, 22]. The initial resistivity values of 5.77 and 6.51 related to λ and V for the Al–Cu–Ti are slightly higher than the initial resistivity values of 4.26 and 4.94 related to λ and V, respectively, for Al–Cu–Ni [21, 22]. As shown in Fig. 5 and Table 2, the ρ value for the Al–Cu–Ti increases from 5.91×10^{-8} Ω m to 12.11×10^{-8} Ω m with the increasing V value from 8.58 μm·s^{-1} to 2038.65 μm·s^{-1}.

The relationships between ρ with λ and V in logarithmic form for the Al–Cu–Ti were determined from linear regression analysis as

$$\rho = 9.106 \times 10^{-8}\,\lambda^{-0.31}, \tag{13}$$

$$\rho = 4.47 \times 10^{-8}\,V^{0.13}. \tag{14}$$

The dependences of ρ on λ and V in logarithmic form obtained in present work were also compared with the dependences of ρ on λ and V in logarithmic form for the Al–Cu–Mg [20], Al–Ni–Fe [21], and Al–Cu–Ni [22] alloys obtained in previous works as shown in Figs. 4 and 5. As shown in Fig. 4 and 5, the lines of ρ versus λ and ρ versus V for the Al–Cu–Ti are slightly above the lines of ρ versus λ and ρ versus V for the Al–Cu–Ni [22], but they are very close to each other in the range of experimental error in ρ measurements.

The exponential 0.13 value of V for the Al–Cu–Ti is in good agreement with the exponential 0.11 and 0.12 values of V for the Al–Cu–Mg [18], the Al–Ni–Fe [19], and the Al–Cu–Ni [21, 22] alloys, respectively. The coefficient value 4.47 of V for the Al–Cu–Ti is very close with the coefficient values 4.13 and 3.48 of V for the Al–Ni–Fe [19] and the Al–Ci–Ni [22], respectively, but the value of 4.47 is nearly

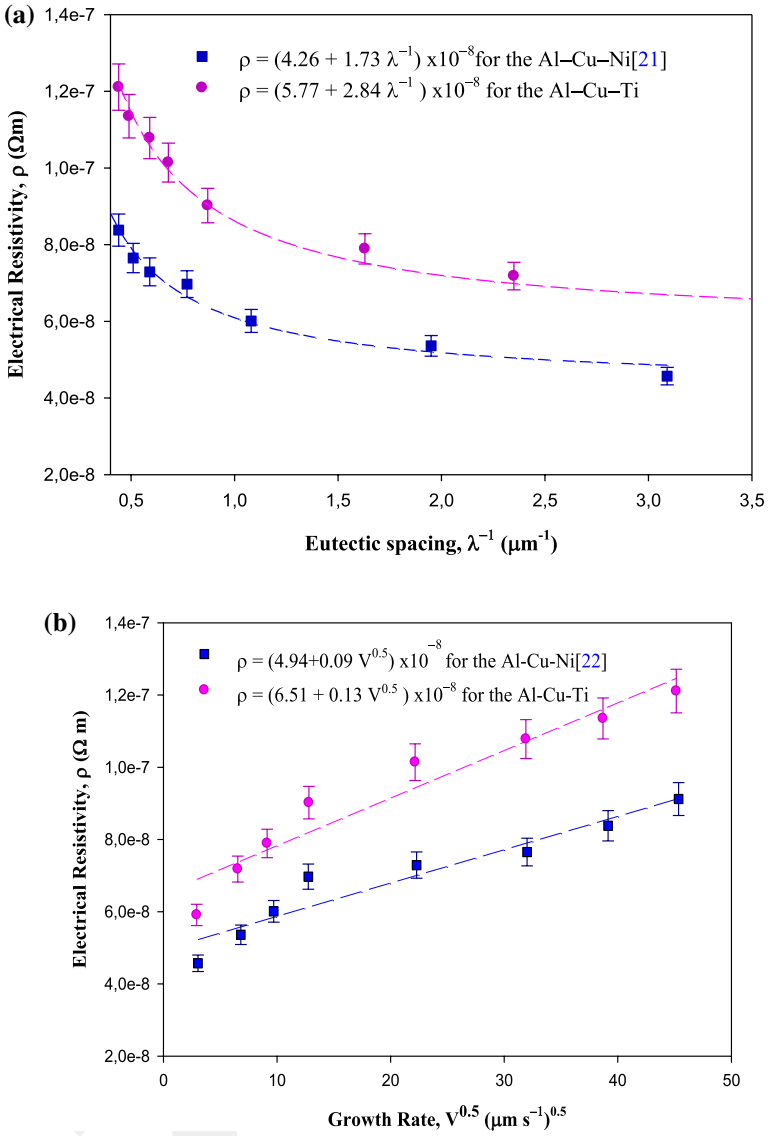

Fig. 4 Variations of ρ with λ and V determined in the form of Hall–Petch-type equation for the Al–Cu–Ni [21, 22] and Al–Cu–Ti eutectic alloys

seven times smaller than 28.82 the coefficient value of V for the Al–Cu–Mg [18]. The ρ values for Al, Cu, Ni, Fe, and Mg are 2.74×10^{-8}, 1.70×10^{-8}, 7.0×10^{-8}, 9.8×10^{-8}, and 4.3×10^{-8} Ω m, respectively, at room temperature [32]. If the values of ρ for the Al–Cu–Ti solidified with the different V values obtained in the present

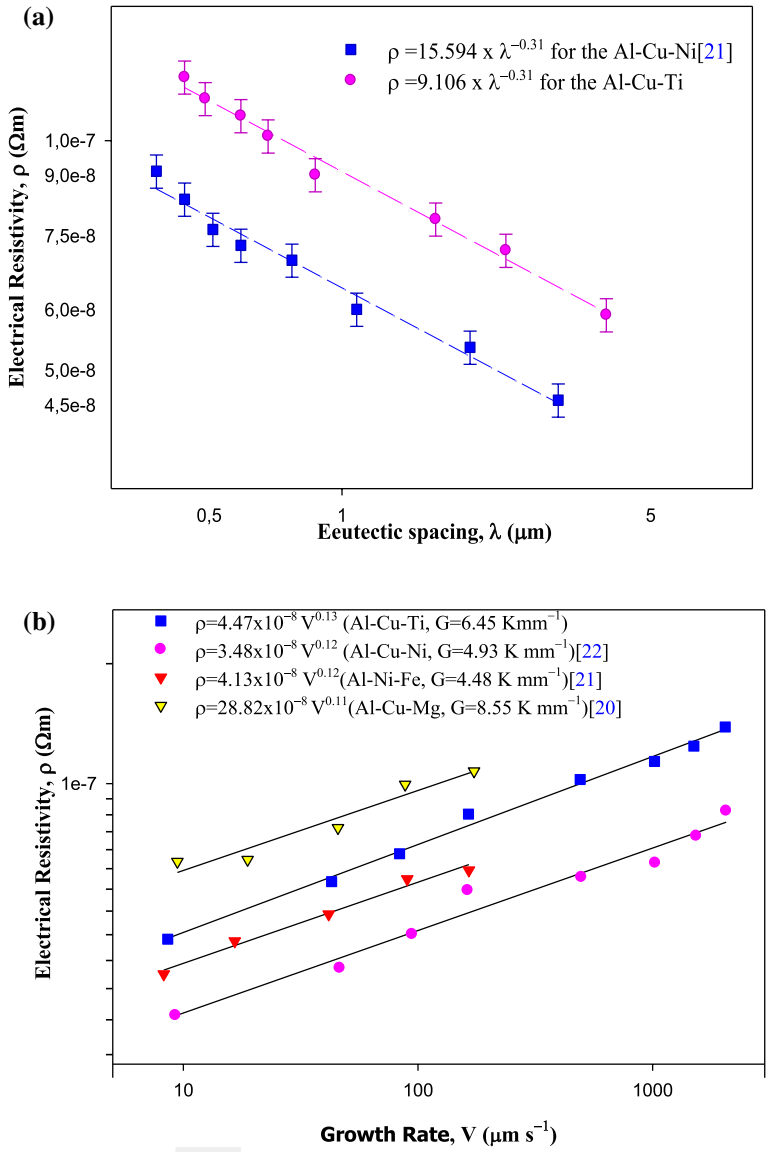

Fig. 5 Variations of ρ with λ and V for directionally solidified Al-based binary or ternary eutectic alloys

work are considered, the disparities in the ρ values arise from the amount and type of alloying elements as well as high growth rates.

3.3 Effect of *V* on *K*

The measured K values for the Al–Cu–Ti solidified with the different V values are given in Table 3 and the K versus T graph of the Al–Cu–Ti's solid phase is shown in Fig. 6. Figure 6 and Table 3 show that the K value linearly increases or decreases with the increasing λ or V values, respectively, and thus, the relationships between them in logarithmic scale for the Al–Cu–Ti alloy were obtained from linear regression analysis as follows:

$$K = 218.89\,\lambda^{0.070}, \tag{15}$$

$$K = 259.95\,V^{-0.031}. \tag{16}$$

A comparison of the K variation with λ and V for the Al–Cu–Ti solidified with different V measured in the present work with the K variation with λ and V for the Al–Cu–Ni [21, 22] is also given in Fig. 6. Figure 6 also shows that the lines of K versus λ and V for the Al–Cu–Ti are superimpose together with the lines of K versus λ and V for Al–Cu–Ni eutectic alloy [22].

The exponential values 0.070 and 0.031 of λ and V for the Al–Cu–Ti are very close to the exponential values 0.091 and 0.037 of λ and V, respectively, for Al–Cu–Ni alloy [21, 22]. The correlation coefficient values 218.87 and 259.96 of λ and V for the Al–Cu–Ti are also very close to the correlation coefficient values 217.17 and 261.64 of λ and V, respectively, for the Al–Cu–Ni [21, 22].

As shown in Table 3, the K values of Al–Cu–Ti solidified with the lowest V (8.58 $\mu m{\cdot}s^{-1}$) and highest V (2038.65 $\mu m{\cdot}s^{-1}$) are obtained as 236.04 $W{\cdot}K^{-1}{\cdot}m^{-1}$ and 199.82 $W{\cdot}K^{-1}{\cdot}m^{-1}$, respectively. The K values for the Al–3 wt%Cu [33], Al–6 wt%Cu [33], Al–15 wt%Cu [33], Al–24 wt%Cu [33], Al [34], Al–33 wt%Cu [35], and Al–52.5 wt. %Cu [35] were measured to be 236 $W{\cdot}K^{-1}{\cdot}m^{-1}$, 186 $W{\cdot}K^{-1}{\cdot}m^{-1}$, 170 $W{\cdot}K^{-1}{\cdot}m^{-1}$, 145 $W{\cdot}K^{-1}{\cdot}m^{-1}$, 135 $W{\cdot}K^{-1}{\cdot}m^{-1}$, 129 $W{\cdot}K^{-1}{\cdot}m^{-1}$, and 105 $W{\cdot}K^{-1}{\cdot}m^{-1}$, respectively, at 300 K. The value of 236.04 $W{\cdot}Km^{-1}$ obtained at

Table 3 The experimental data in the measurements of K versus V in Al–33 wt% Cu–0.1 wt% Ti eutectic alloy at 300 K

Growth rate, V ($\mu m{\cdot}s^{-1}$)	Net heat transfer rate trough to sample, Q(W)	Temperature difference into sample, ΔT (K)	Thermal conductivity, K ($W{\cdot}K^{-1}{\cdot}m^{-1}$)
8.58	2.23	2.25	236.04 ± 21.24
42.85	0.64	0.66	232.39 ± 20.92
83.42	1.50	1.55	230.74 ± 20.76
164.15	1.59	1.69	224.02 ± 20.16
490.81	1.56	1.68	221.43 ± 19.93
1018.16	1.38	1.57	209.80 ± 18.88
1497.42	2.23	2.64	202.24 ± 18.20
2038.65	1.58	1.89	199.82 ± 17.98

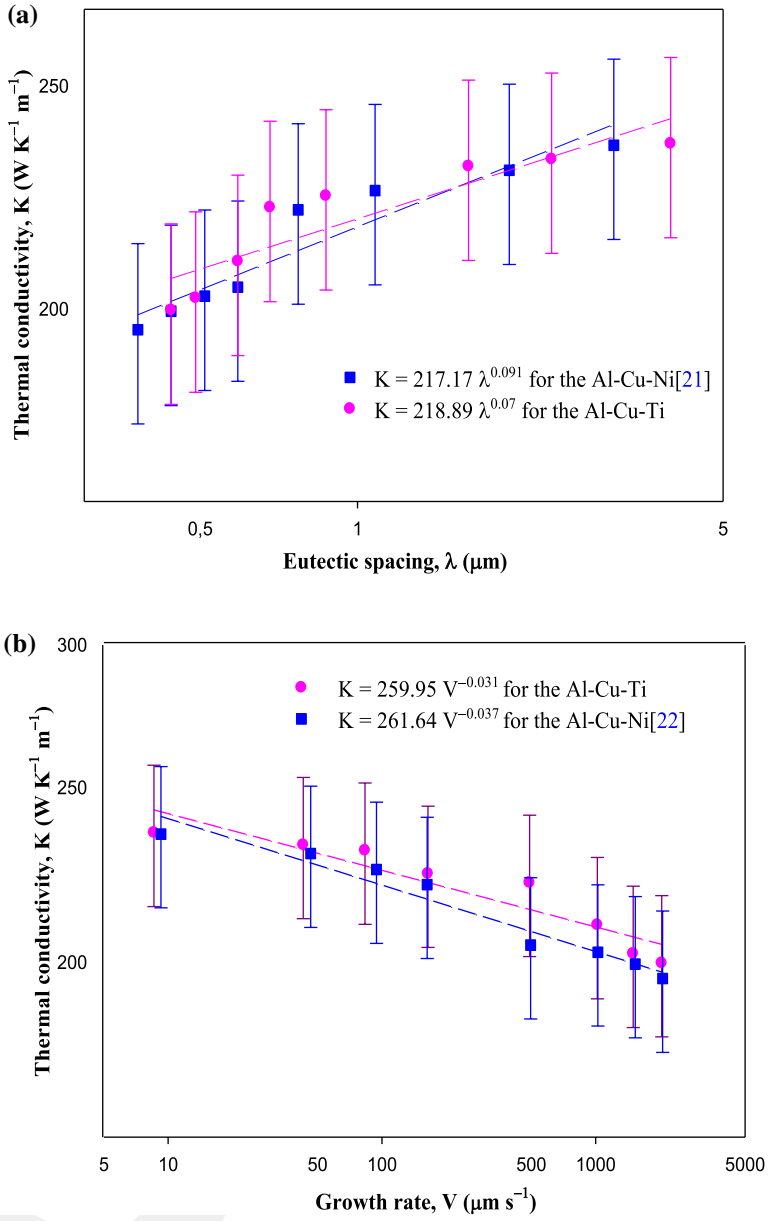

Fig. 6 Variations of K with λ and V for the Al–Cu–Ni [21, 22] and Al–Cu–Ti eutectic alloys

the growth rate of 8.58 μm·s^{-1} is close the K value of 236 W·K^{-1}·m^{-1} for Al [34]. The value of 199.82 W·K^{-1}·m^{-1} for 2038.65 μm·s^{-1} is slightly higher than the values of K for cast Al–Cu alloys [33–35]. In previous works [33–35], the specimen for K measurements was prepared as a cast alloy, i.e., the molten alloy into the crucible

solidified under transient growth condition, i.e., the V value varies with time during the solidification processes and the V value is higher than the highest V value for directional solidification procedure. Therefore, the grain sizes in cast alloys are smaller and the microstructures are different from the microstructure of directional solidified alloys. In directional solidified samples, the grain sizes are larger and phase structure is uniform and regular according the grain size and microstructures in cast alloys. Thus, the ρ values for alloy directional solidified with a constant V should be smaller than the ρ values of cast alloy prepared under transient growth conditions. Therefore, this dissimilarity between the K values measured in the present work and K values measured in previous works for the Al–Cu alloy arises from the sample preparation under different conditions.

The relationship between the K and ρ is established by the Wiedemann–Franz law, which is based upon the fact that heat and electrical transport both involve the free electrons in the metal as

$$K\rho = LT, \tag{17}$$

where L is the Lorenz number. The theoretical value of Lorenz number for metals is 2.45×10^{-8} W·Ω·K^{-2} [36]. The variations of L with V were determined from the Wiedemann–Franz law and are also given Table 2. As shown in Table 2, the value of L increases from 4.65×10^{-8} W·Ω·K^{-2} to 8.07×10^{-8} W·Ω·K^{-2} with the increasing value of V from 8.58 μm·s^{-1} to 2038.65 μm·s^{-1}.

Recent developments on additive manufacturing of precision optics at micro- and nanoscale were reviewed by Zolfaghari et al. [37]. Laser-induced melting and solidification process can be considered as directional solidification. All results and discussion obtained on the V effects on K and ρ in the Al–Cu–Ti eutectic alloy can be extended to the V effects on K and ρ in laser-induced melting and solidification when the driving velocity of laser beam is chosen to be in the range of 8.58 μm·s^{-1} to 2038.65 μm·s^{-1}.

3.4 Determinations of ΔC_p and ΔH of Fusion for the Al–Cu–Ti Eutectic Alloy

The Al–Cu–Ti alloy was heated with a heating rate of 10 K·min^{-1} from 300 K to 1000 K by using a Perkin Elmer Diamond model *DSC* and the temperature versus heat flow trace is shown in Fig. 7 for the Al–Cu–Ti. The melting temperature of Al–Cu–Ti was determined as 837.13 K from the cooling trace shown in Fig. 7. The values of ΔH and ΔC_P for the Al–Cu–Ti were determined to be 222.69 J·g^{-1}, and 0.266 J·g^{-1}·K^{-1} and they are very close to the values of 204.8 J·g^{-1}, 0.374 J·g^{-1}·K^{-1} and 223.8 J·g^{-1}, 0.433 J·g^{-1}·K^{-1} for Al–23.9wt%Cu–1.2wt%Co [16] and Al–17.6wt%Cu–42.2wt%Ag [17] alloys, respectively.

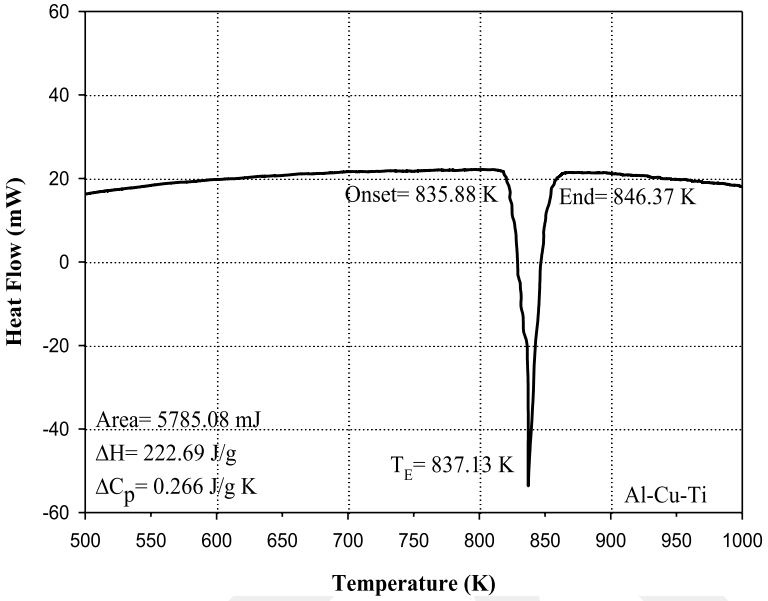

Fig. 7 Heat flow curve versus the temperature for Al–33wt% Cu–0.1wt% Ti at a heating rate of 10 K·min^{-1}

4 Conclusions

The microstructure of Al–33.0wt%Cu–0.1wt%Ti has fine cellular eutectic with the increasing value of V. The highest and the lowest values for λ were determined as 3.97 ± 0.48 μm and 0.44 ± 0.05 μm at 8.58 μm·s^{-1} and 2038.65 μm·s^{-1}, respectively. Dependences of ρ on λ and V were determined in the form of H–P and from linear regression analysis for the Al–Cu–Ti. Influences of V and λ on K in the Al–Cu–Ti were also investigated and the highest and lowest K values were obtained as 236.04 and 199.82 W·K^{-1}·m^{-1} with the V value of 8.58 and 2038.65 μm·s^{-1}, respectively. The line of ρ versus V for the Al–Cu–Ti is very close to the line of ρ versus V for Al–Cu–Ni eutectic alloy [22] and the lines of K versus V for the Al–Cu–Ti and Al–Cu–Ni [22] are superimposed to each other. From the plot of heat flow versus temperature, the values of ΔH and ΔC_p and the melting temperature for the Al–Cu–Ti were found to be 222.69 J·g^{-1}, 0.266 Jg^{-1}·K^{-1}, and 837.13 K, respectively.

Acknowledgments This work was supported by Erciyes University Scientific Research Project Unit under Contract No: FDK-2013-4741. The researchers are thankful to Erciyes University Scientific Research Project Unit for their financial supports.

Declarations

Conflict of interest The authors claim that they have no conflict of interest.

References

1. J. Auchet, J.L. Bretonnet, Rev. Int. Hautes Temper. Refract. **26**, 181 (1990)
2. H. Jones, W. Kurz, Z. Metallkunde **4**, 792 (1981)
3. Y.S. Sun, G.W. Lorimer, N. Ridley, Metall. Trans. **21A**, 575 (1990)
4. I. Ziv, F. Weinberg, Metall. Trans. B. **20B**, 731 (1989)
5. C.Y. Wang, C. Beckermann, Metall. Mater. Trans. A. **25A**, 1081 (1994)
6. H.B. Dong, P.D. Lee, Acta Mater. **53**, 659 (2005)
7. M. Rhême, F. Gonzales, M. Rappaz, Scripta Mater. **59**, 440 (2008)
8. W.R. Osório, J.R. Spinelli, N. Cheung, A. Garcia, Mater. Sci. Eng. A **420**, 179 (2006)
9. J. De Wilde, L. Froyen, S. Rex, Scripta Mater. **51**, 533 (2004)
10. K.A. Jackson, J.D. Hunt, Trans. Metall. Soc. AIME **236**, 1129 (1966)
11. D.M. Stefanescu, G.J. Abbaschian, R.J. Bayuzick, *Solidification Processing of Eutectic Alloys* (Metallurgical Society Inc., Pennsylvania, 1989), pp. 4–8
12. A. Ourdjini, L. Liu, R. Elliott, Mater. Sci. Technol. **10**, 312 (1994)
13. S. M. D. Borland, R. Elliott, Metall. Trans. A **9**, 1063 (1078)
14. M. Asta, C. Beckermann, A. Karma, W. Kurz, R. Napolitano, M. Plapp, G. Purdy, M. Rappaz, R. Trived, Acta Mater. **57**, 941 (2009)
15. H. Kaya, E. Çadırlı, M. Gündüz, J. Mater. Process. Technol. **183**, 310 (2007)
16. E. Çadırlı, İ Yılmazer, M. Şahin, H. Kaya, Trans. Indian Inst. Met. **68**, 817 (2015)
17. U. Böyük, N. Maraşlı, H. Kaya, E. Çadırlı, K. Keşlioğlu, Curr. Appl. Phys. **12**, 7 (2012)
18. Y. Kaygısız, N. Maraşlı, Phys. Metals Metall. **118**, 389 (2017)
19. S. Engin, U. Böyük, N. Maraşlı, J. Alloys Compd. **660**, 23 (2016)
20. Ü. Bayram, N. Maraşlı, Metall. Mater. B **49B**, 3293 (2018)
21. Ü. Bayram, Investigation of The Dependence of Mechanical, Electrical and Thermal Properties with Structure Parameters on The Growth Rates in The Directionally Solidified Aluminium and Zinc Based Multi Components Alloys (D. Ph. Thesis, Erciyes University Kayseri-Turkey 2013) pp. 145–156
22. Ü. Bayram, N. Maraşlı, J. Alloys Compd. **753**, 695 (2018)
23. V. Rudnev, D. Loveless, R. Cook, M. Black, *Handbook of Induction Heating* (Markel Dekker Inc., New York, 2003), pp. 119–120
24. L.B. Valdes, Proc. IRE. **42**, 420 (1954)
25. M. Şahin, E. Çadırlı, Ü. Bayram, P. Ata Esener, J. Thermal Anal. Calorim. **132**, 317 (2018)
26. J. B. Biot, Traite de Physique 4 (Paris 1816) p. 669
27. J. B. J. Fourier, The Analytical Theory of Heat (Gauthier-Villars, Paris 1822,; English translation by Freeman, A. Cambridge University Press,1878; new edition of the English translation, Dover Publication; New York 1955) p. 466
28. S. Aksöz, E. Öztürk, N. Maraşlı, Measurement **46**, 161 (2013)
29. S. Akbulut, Y. Ocak, K. Keşlioğlu, N. Maraşlı, J. Phys. Chem. Solids **70**, 72 (2009)
30. Materials Science International Team, Light Metal Systems (Part 2 Volume 11A2, the series Landolt-Börnstein-Group IV Physical Chemistry Al-Cu-Ni, Aluminium-Copper-Titanium 2003) pp. 156–173
31. V.S. Zolotorevsky, N.A. Belov, M.V. Glazoff, *Casting Aluminium Alloys* (Elsevier, Pittsburgh, 2007), pp. 34–35
32. G. T. Meaden, Electrical Resistance of Metals (International Cryogenics Monograph Series. Chapter 1 Springer Science- Business Media, France, LLC 4 1965) pp. 12–58
33. S. Aksöz, Y. Ocak, N. Maraşlı, E. Çadırlı, H. Kaya, U. Böyük, Exp. Thermal Fluid Sci. **34**, 1507 (2010)
34. Y.S. Touloukian, R.W. Powell, C.Y. Ho, P.G. Klemens, *Thermal Conductivity Metallic Elements and Alloys* (IFI Plenum, New York, 1970), pp. 1–8
35. M. Gündüz, J.D. Hunt, Acta Mater. **33**, 1651 (1985)
36. C. Kittel, *Introduction to Solid State Physics*, 6th edn. (Wiley, New York, 1965), pp. 152–153
37. A. Zolfaghari, T.T. Chen, A.Y. Yi, Int. J. Extrem. Manuf. **1**, 012005 (2019)